

Effective blood vessels reconstruction methodology for early detection and classification of diabetic retinopathy using OCTA images by artificial neural network

Mohamed M. Abdelsalam

Computers and Systems Dep, Faculty of Engineering, Mansoura University, 35516, Egypt



ARTICLE INFO

Keywords:

Diabetic retinopathy
Optical coherence tomography angiography
Artificial intelligence
And artificial neural network classifier

ABSTRACT

Background: Diabetic retinopathy (DR) refers to the ocular effect of diabetes. It is one of the retinal vascular diseases that can cause loss of vision. DR leads to alterations in vascular networks, including angiogenesis and capillary regression.

Objective: The objective of this research is to provide an effective robust and accurate automatic methodology for the early detection of DR subjects. The methodology depends on two steps: 1) Blood vessel reconstruction, enhancement, and re-continuity using written custom programs, and 2) An Artificial Neural Network (ANN) as an automatic classifier between the diabetic without diabetic retinopathy (DR) and the Mild to Moderate Non-Proliferative Diabetic Retinopathy (NPDR) subjects.

Methods: This approach depends on extracting the seven features, which are the most changeable features according to the morphological retinal vascular network changes. These features are the mean of the intercapillary areas as regions of interest for the largest 10 and 20 selected regions, either including or excluding the Foveal Avascular Zone (FAZ) region, FAZ perimeter, circularity index, and vascular density. The OCTA images were obtained and approved by the Ophthalmology Center in Mansoura University-Egypt.

Results: One hundred images were processed, distributed as follows: 40 eyes were normal, 30 eyes were diabetic without DR, and 30 eyes were NPDR subjects. The total system accuracy reached 97%. The performance parameters of the classification system for normal versus diabetic were 97.5% for sensitivity, 96.67% for specificity, and 95.2% for precision. While, the measures for a diabetic without DR versus non-proliferative DR (mild to moderate) were 96.67% for sensitivity, 96.67% for specificity, and 96.67% for precision. The maximum misclassification error was 3.33%.

Conclusion: The proposed methodology is capable of accurate classification of the diabetic without DR and Non-proliferative diabetic retinopathy subjects. This methodology depends on using written custom programs and a plugin for MATLAB and Fiji based Image-J software with a supervised artificial neural network. This technique achieves high accuracy, resolution, specificity, and precision with only a short time needed for diagnosis.

1. Introduction

Artificial Intelligence (AI) garnered attention as a healthcare assistant in detection, classification, diagnosing, and extracting information from images in the analysis of medical systems [1]. AI uses complex algorithms and software to simulate the human brain for information processing and decision-making. Most applications of AI in medicine can be summarized as follows:

- 1) *Diagnosis of Diseases:* AI supports doctors in diagnosis, since the availability of patient symptoms and/or imagery are collected and

processed by algorithms and techniques assisting clinical practice. To improve AI accuracy, it can be equipped with learning and self-correcting abilities based on feedback. This improvement improves automatic diagnoses as well as making diagnostics processes less expensive and more accessible [2,3]. Artificial intelligent techniques were used in diagnosing several diseases related to neoplasms [4–6], nervous [7,8], retinopathy [9–11], cardiovascular [12–14], urogenital [15,16], pregnancy [17,18], digestive [19,20] and respiratory [21,22].

- 2) *Discovery and Development of Drugs:* Drug development and discovery is an expensive process. AI plays a major role as it, can predict the

E-mail addresses: E-mail address: mohmoawed@yahoo.com. mohmoawad@mans.edu.eg.

<https://doi.org/10.1016/j imu.2020.100390>

Received 23 May 2020; Received in revised form 25 June 2020; Accepted 30 June 2020

Available online 1 July 2020

2352-9148/© 2020 The Author. Published by Elsevier Ltd. This is an open access article under the CC BY-NC-ND license

(<http://creativecommons.org/licenses/by-nc-nd/4.0/>).

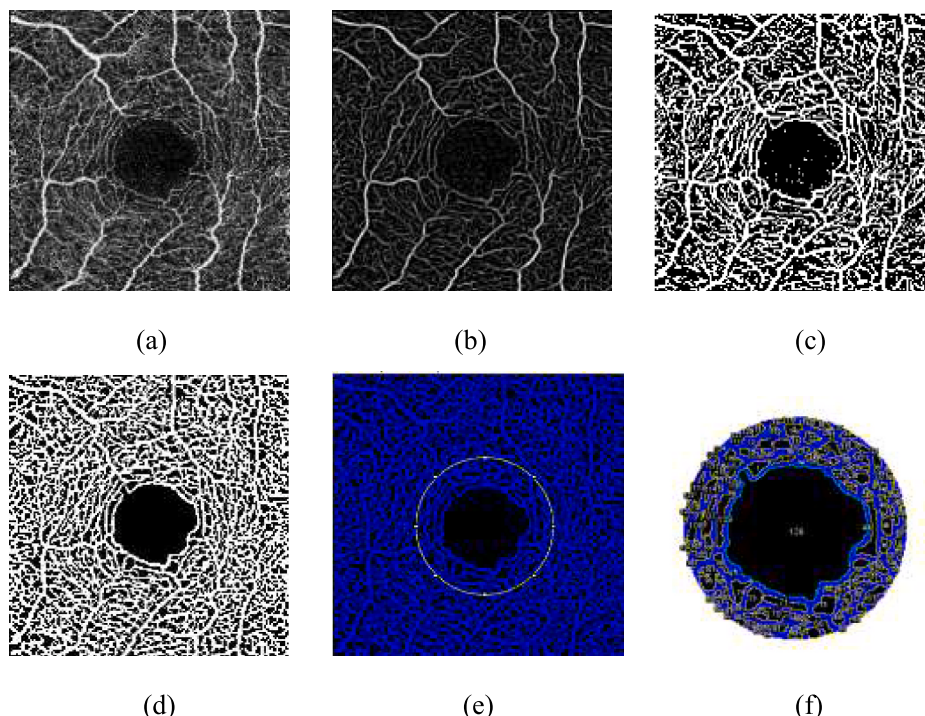


Fig. 1. The image processing steps (a) Source OCTA image (b) The single detailed microvascular structure image with resolution enhancement (c) Binarized image with vessels reconstruction (d) A circle with 1.5 mm centered at FAZ region (e) calculate the designed intercapillary areas lie inside the circle.

behavior of the molecules and how they can be combined to make a useful drug. The biopharmaceutical companies use AI for analyzing biological data, identifying targets, and searching for varieties that lead to more effective drug discovery [23].

- 3) **Personalized treatment:** Responding to drugs and treatment schedules may differ from one patient to another. Therefore, personalized treatment has become the main potential to enhance patient lifespan [24]. But it is difficult to determine the appropriate method of treatment for each individual patient. Hence, with the availability of patients' data and their medical history, AI algorithms can perform a complicated statistical analysis to predict the response of a particular patient treatment.
- 4) **Improve gene editing:** AI algorithms and computer models identify patterns within genetic datasets and they can predict patient disease progression, intervention response, or the impact of a gene mutation [25].

Diabetes is a group of metabolic diseases characterized by hyperglycemia, while diabetic retinopathy (DR) refers to the effect of diabetes in the eye. DR is one of the retinal vascular diseases that cause loss of vision [26,27]. When the sugar ratio permanently increases in the blood, it blocks the tiny blood vessels to the retina in the human eye; it causes bleeding or fluid leakage from these vessels. Therefore, the eyes grow vascular abnormalities with neovascularization on the retina surface, but this neovascularization almost does not work well and causes hemorrhage [28]. In the early stages, no changes in vision are observed. But with time, diabetic retinopathy causes vision loss [29,30]. Hence, the early detection of DR and timely treatment prevent or delayed diabetic-related blindness [31].

According to the International Clinical Diabetic Retinopathy Disease Severity Scale, diabetic retinopathy can be classified into: 1) **Non-Proliferative Diabetic Retinopathy (NPDR)**, which in turn is classified into a) *Mild NPDR*: in this case, the retina has fewer microaneurysms, with no change in the vision. b) *Moderate NPDR*: is more than microaneurysms but it is less than Severe NPDR. c) *Severe NPDR*: the patients suffer from any of the following: more than 20 intraretinal hemorrhages, definite

venous bleeding, and prominent intraretinal microvascular abnormalities (IRMA). Consequently, many blood vessels, which cause abnormal growth factor secretion, are blocked. 2) **Proliferative Diabetic Retinopathy (PDR)**: is the advanced stage in which patients suffer from neovascularization and vitreous/preretinal [32].

The diagnostic algorithms depend on the retinal medical imaging methods, which can be classified according to invasive or non-invasive image techniques into: 1) **Invasive techniques**: Fluorescein Angiography (FA) and Indocyanine Green Angiography (ICGA), which require up to 10–30 min of intravenous dye administration and imaging. They provide 2D images of dynamic visualization of blood flow through retinal vessels [33,34]. 2) **Non-invasive techniques**: the Optical Coherence Tomography Angiography (OCTA) is the latest non-invasive technique [35–37]. It provides volumetric blood flow information images by the reflectance of laser light on the surface of moving red blood cells to depict vessels accurately through different segmented areas of the eye.

Several researchers introduced different classifications and detection methods of diabetic retinopathy for early diagnosis and treatment. In Ref. [38], they proposed an algorithm based on a combination of image processing techniques as the Circular Huge Transform (CHT) and Contrast Limited Adaptive Histogram Equalization (CLAHE). In special issues [39], they used a Gabor filter for classification of normal and abnormal fundus images. Different Image preprocessing methodologies were used for RGB retinal fundus image with Adaboost, Gradientboost, RandomForest, and Voting classifiers of DR and normal patients. In Refs. [40], they proposed a system for extracting the fovea, optic disc, and retinal tissue for dark spot lesions segmentation in the fundus images. The classification system is based on the number and location of microaneurysms and hemorrhages.

Microaneurysms were extracted from RGB Fundus images by using three techniques - Illumination equalization, CLAHE, and Smoothing. In low brightness and poor contrast regions, microaneurysms are hardly visible [41]. A deep learning algorithm is employed for DR classification either by using features extracting methods [42] or using retinal fundus dataset images [43–47]. Convolutional Neural Networks (CNNs) have been successfully applied to classify DR. In Ref. [48], the authors used

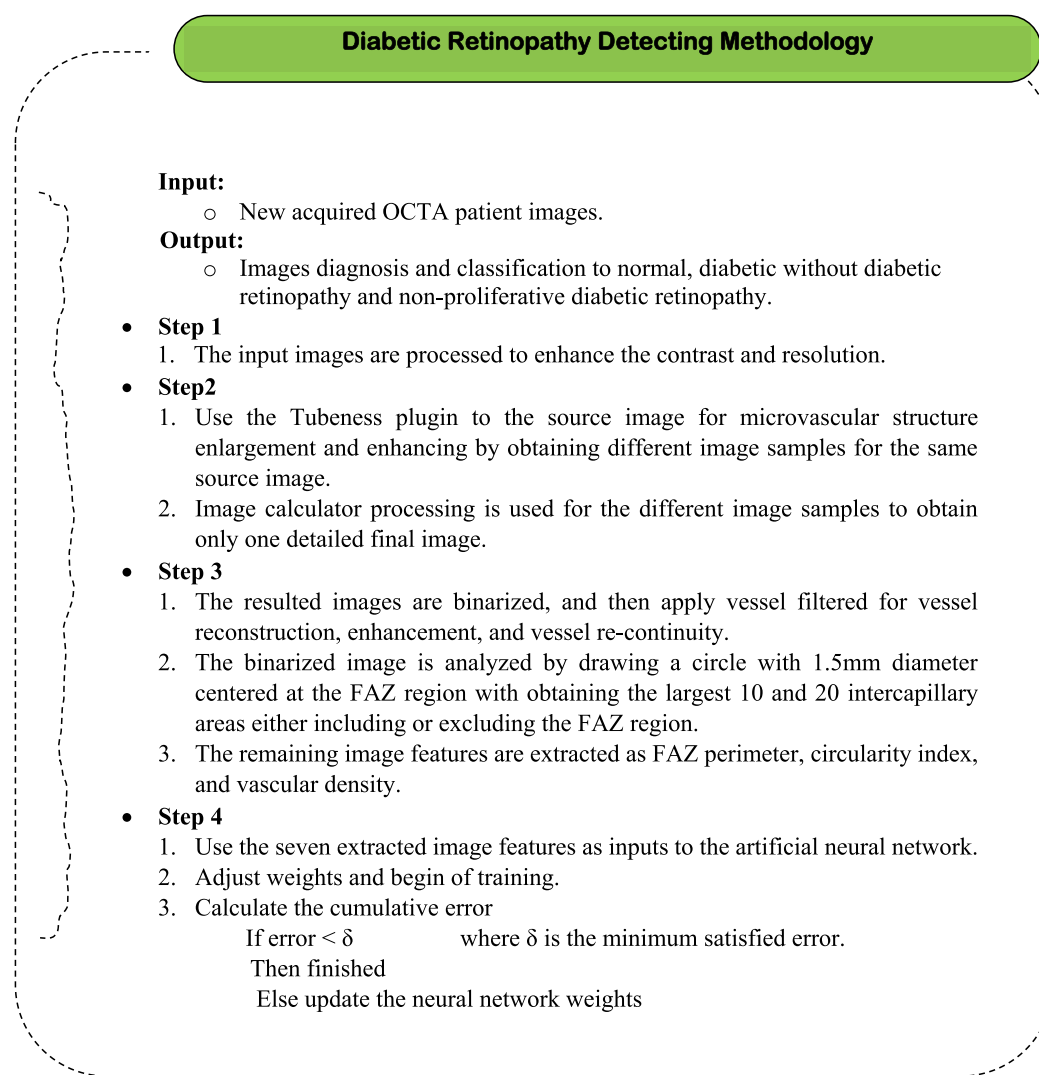


Fig. 2. Diabetic retinopathy detecting methodology.

CNNs on color fundus images using pre-trained GoogLeNet and AlexNet models with two available datasets containing approximately 36200 images. Another CNNs training method based on an open-source numerical computation library for Python was applied on fundus images [49], with datasets over 30000 images. Moreover [50–52], the authors used CNN for DR classification using color fundus images available in the Kaggle dataset with over 80000 dataset images.

A k-means color compression technique was used to cluster fundus images to differentiate regions of interest, and then diabetic parts were segmented out; finally, DR was recognized by a knowledge-based fuzzy inference system (FIS) [53]. In Refs. [54], they proposed a framework for the analysis of retinal vascular geometric features. Retinal fundus images were segmented and the geometric features were extracted for the classification model, which is based on statistical inferences.

Neural networks have attracted the attention of many researchers [55,56]. A dual classification approach is used for new blood vessels. Morphology, intensity and gradient-based features created a 21-D feature set. Thereafter, a genetic algorithm was used for feature selection and SVM (Support Vector machine) parameter selection [57].

Early detection is the main objective of this study for preliminary treatment that can prevent or delay diabetic-related blindness. An automatic algorithm for detection and classification of normal, diabetic without diabetic retinopathy and Non-Proliferative diabetic retinopathy (Mild and Moderate) is proposed. The algorithm can be extended easily

for the detection of other stages like severe NPDR and PDR. However, this study aims at detecting the early stages, which may be confused at times based on the quality of the images or multiple diagnoses to make the appropriate decision. The input images were obtained and approved from Ophthalmology Center in Mansoura University - Egypt and they were imaged by Triton Topcon Swept-Source OCTA.

1.1. Research contributions

The research contributions are as follows:

- 1) Most of the researches designed their classification techniques based on CNN using retinal fundus images. Which indeed needs large datasets for network training, lack of depth appreciation on images, and less magnification for capillaries. While, the OCTA approach provides a quantitative analysis of the retinal vessels with detailed information about retinal microvasculature.
- 2) The proposed technique for blood vessel reconstruction and re-continuity uses developed written programs and plugin for MATLAB and Fiji-ImageJ software. Rather than the usage of standard available functions, which had not good results in case of low image resolution or quality.
- 3) Extracting the seven features, which are the most changeable features according to the morphological retinal vascular network

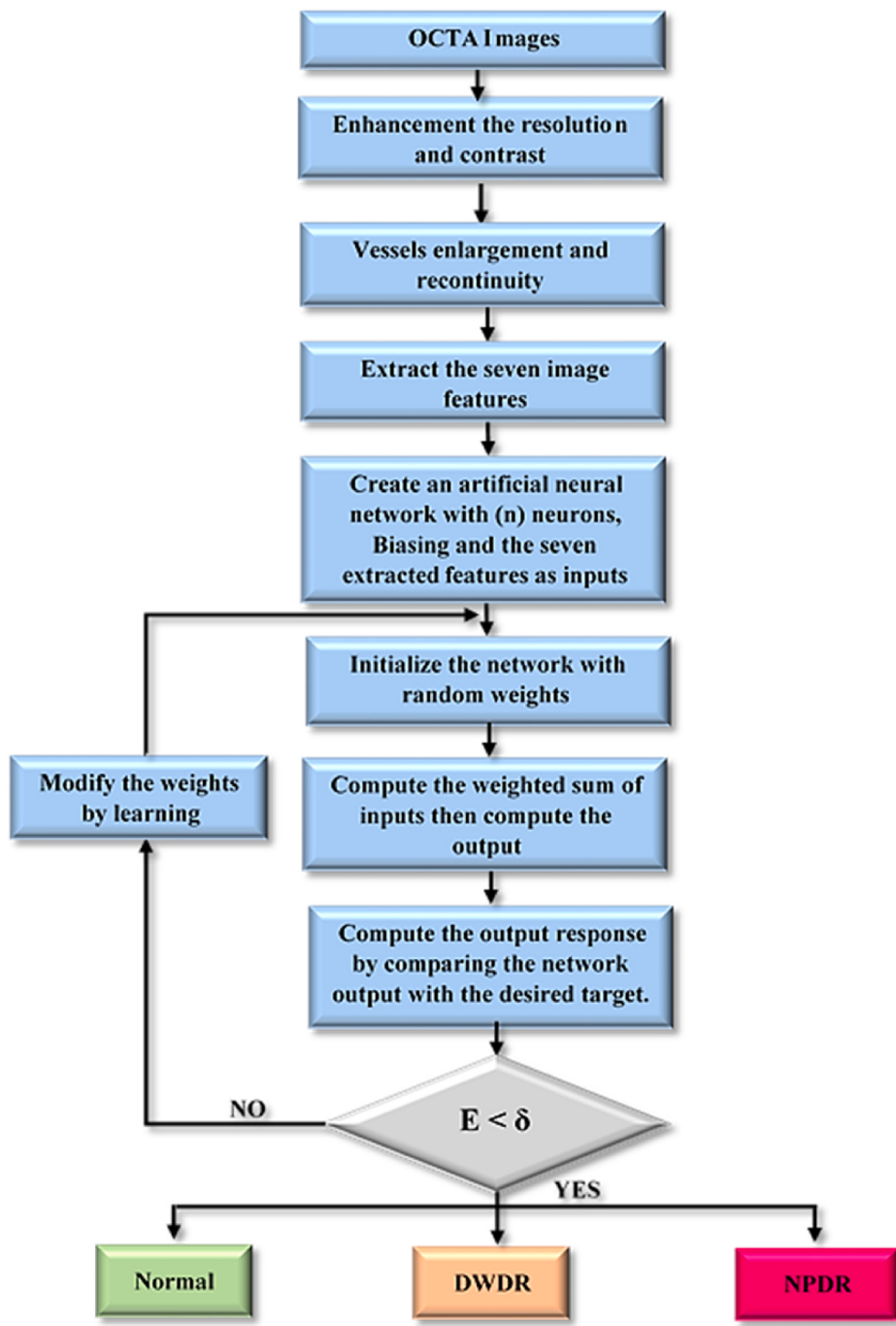


Fig. 3. The proposed methodology flowchart.

changes. These features are the mean of the intercapillary areas as regions of Interest (ROI) for the largest 10 and 20 selected regions, either including or excluding the FAZ region, FAZ perimeter, circularity index and vascular density.

4) The resulted divergent numerical datasets are used to train the supposed ANN. The suggested methodology achieved 97% accuracy.

2. Material

2.1. Patient retinal image

The retrospective observational case series were obtained and approved by Ophthalmology Center - Mansoura University - Egypt. The sample, in this study, can be classified into 40 eyes of healthy persons,

30 eyes of diabetic ones without DR, and 30 eyes of NPDR persons. The subjects ranged between 40 and 65 years old. All subjects were determined via clinical examination by a retinal specialist.

2.2. OCTA imaging

All subjects underwent imaging on (Triton Topcon Swept-Source OCTA). Topcon Medical Systems (TMS), based in Oakland, NJ, is a leading developer and supplier of diagnostic equipment for the ophthalmic community. Topcon Medical Systems is a wholly-owned subsidiary of Topcon Corporation of Tokyo, Japan.

The device has features such as acquisition speed of 100,000 A-scans/sec, 1050 nm wavelength, the separated B-scan acquisition time approx. 14 msec? It automatically detects 7 boundaries including the

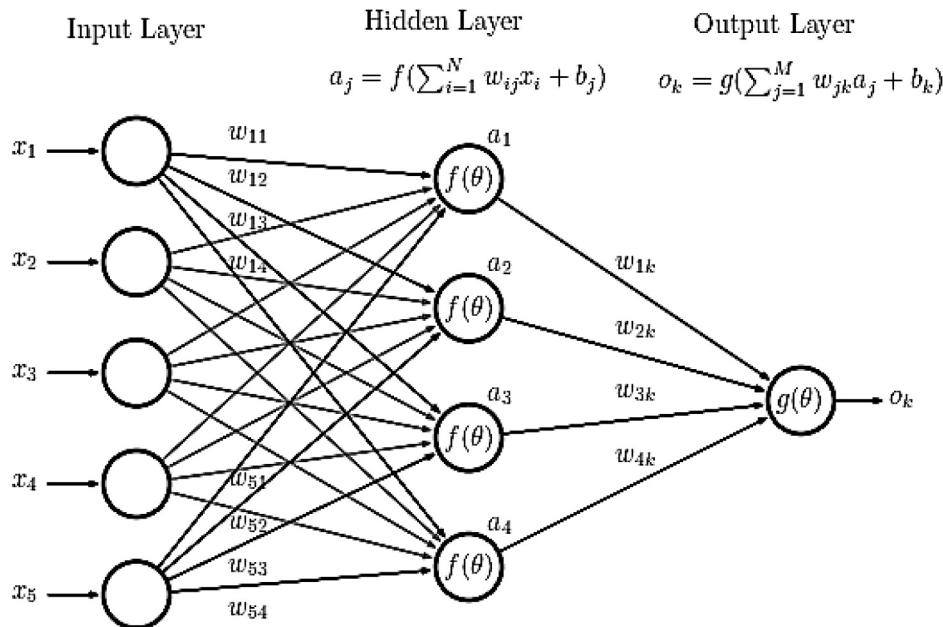


Fig. 4. Multilayer artificial neural network.

chorio-scleral interface. The 12 mm B-scan covers both the macular area and the optic disc [58].

The device has en-face acquisition areas with 3*3 mm, 4.5*4.5 mm, and 6*6 mm. The studied images were performed using angiographic 3*3 mm for more retinal vascular system details. Scan pattern consists of 4 repeated B-scans of 320 A-scans each at 320 raster positions, centered at the fovea center. The theoretical acquisition time for 320*320 A-scans is 4.1 s.

Some of the obtained images suffer from artifacts like low resolution, cut in the image because of the patient's movement or eye blinking, and the FAZ location not centered in the image. These artifacts will be illustrated in the following studied images.

3. Methods

3.1. Diabetic retinopathy detection method

The image processing technique steps can be illustrated in Fig. 1. The methodology based on a machine learning method can be discussed as follows:

1. The input images were 320 × 320 pixels in grayscale. The source image may suffer from low resolution, less quality, and inability to detect blood flow through blood capillaries or microvascular blood vessels. As it is shown in Fig. 1-a.
2. A custom program was written using MATLAB software for contrast and resolution enhancement. Firstly, a threshold value was used for showing the microvascular structure pixels. Secondly, obtainment of the grayscale matrix for the image pixels has been done. Omitting the stand-alone pixels without any near neighbor pixels and adjusting the background image color.
3. Multistage "Tubeness" plugin is a modified written plugin using Fiji/ ImageJ software. It was used for microvascular structure enlargement by obtaining different image samples for the same source image with different vessel diameters.
4. Combine the different image samples to obtain a single detailed microvascular structure image as in Fig. 1-b.
5. Binarization vessel maps were constructed. They were performed by scanning the image pixels starting at the border of the image towards

the neighboring pixels with pixels conversion that has values above an empirically pre-defined threshold as shown in Fig. 1-c.

6. Vessels reconstruction and re-continuity were performed by using a custom-written MATLAB program to obtain Fig. 1-d.
7. Finally, the FAZ region is defined as the largest continuous area inside the central border of the capillary network, which was outlined automatically. And then, drawing a circle with radius 1.5 mm is centered at the FAZ region as in Fig. 1-e.
8. Calculating the required intercapillary areas as illustrated in Fig. 1-f, and beginning to extract the other desired features.
9. Creating an ANN with four layers for DR classification. The network consists of an input layer with seven neurons, which are the seven extracted features. Two hidden layers with 5 and 10 neurons respectively. One output layer with three neurons for the three classification stages. The network was trained until reaching the minimum satisfied error (δ). Where the minimum satisfied error is selected as 10^{-4} .

The Diabetic retinopathy detection methodology is shown in Fig. 2.

3.2. The image extracted features

Drawing a circle with diameter 1.5 mm centered at the FAZ region, and then extract the seven features as follows:

1. The mean of the largest 10 intercapillary areas as regions of interest that surround the FAZ region and lie inside the circle, excluding the FAZ region area.
2. The mean of the largest 20 intercapillary areas as regions of interest that surround the FAZ region and lie inside the circle, excluding the FAZ region area.
3. The mean of the largest 10 intercapillary areas that surround the FAZ region and lie inside the circle, including the FAZ region area.
4. The mean of the largest 20 intercapillary areas that surround the FAZ region and lie inside the circle, including the FAZ region area.
5. FAZ perimeter, which is the length of the blood vessels surrounding the FAZ region.
6. FAZ circularity index, which is a measure of the perfect circularity shape. The perfect circularity shape leads to circularity index equal

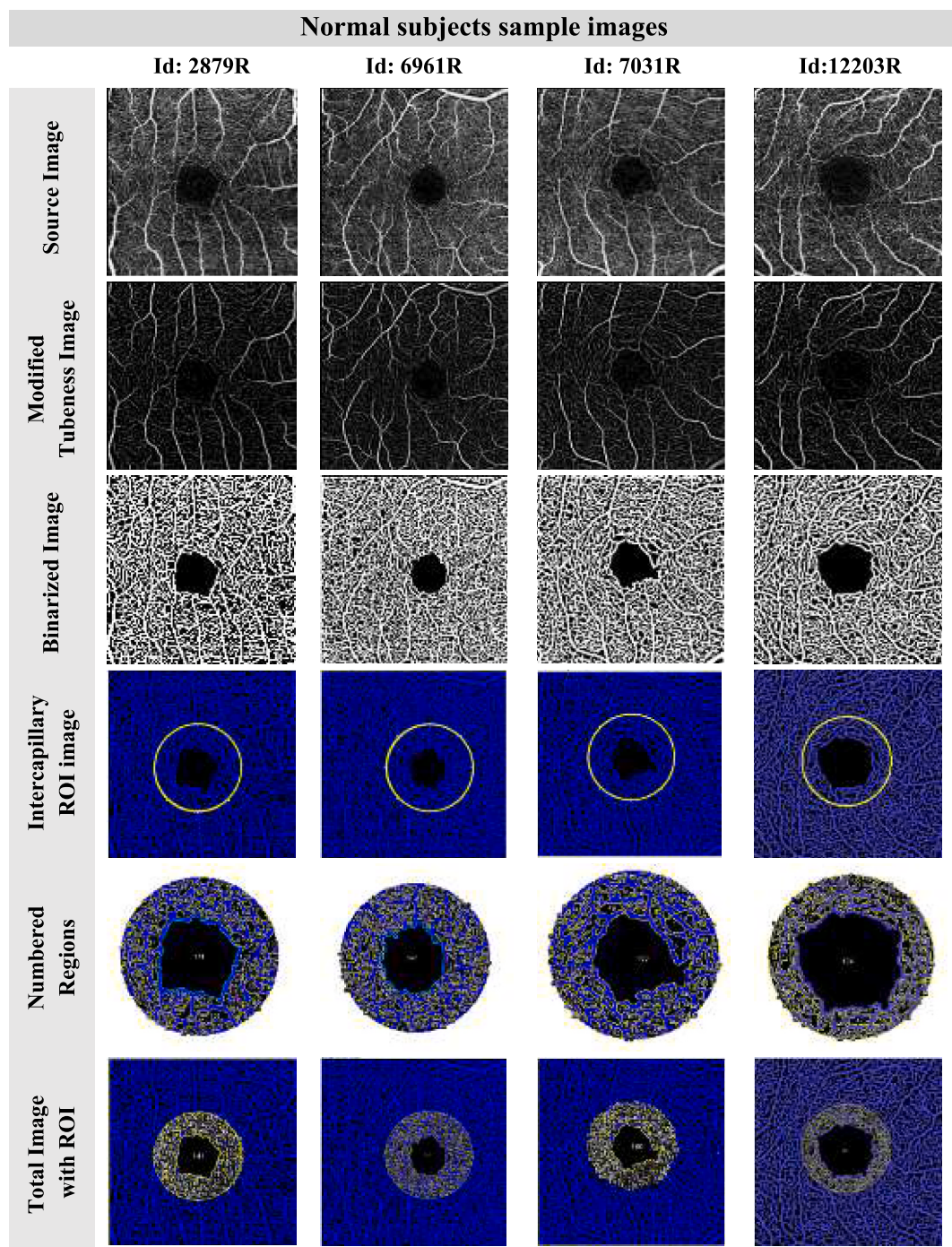


Fig. 5. Normal subjects Sample Images.

1; irregular circularity shape has a value less 1. Instead, some researches calculate the acircularity index [59].

7. Vessel density for the whole image.

Then apply the seven extracted features as neural network inputs and begin the network training. All these steps are summarized in the flowchart of the proposed methodology, which is shown in Fig. 3.

3.3. Artificial neural network in brief

Neural Networks are a set of algorithms modeled closely to the human brain; they are designed to perform almost nonlinear statistical modeling. ANN is a biologically inspired programming paradigm, which

enables a computer to learn from observational data. It is the most commonly used method for developing predictive models for dichotomous outcomes in medicine. The basic element in the network architecture is called a neuron, which performs a specific task according to its activation function. The basic architecture consists of three types of neuron layers: input, hidden, and output layers as shown in Fig. 4.

Where a_j is the output of a j th neuron in the hidden layer, o_k is the network output, $\omega_{i,j}$ is the network weight for the path (i,j) and b_j is the j th neuron bias. In feed-forward networks, the signal flow is from input to output units, strictly in a feed-forward direction. The objective of training the neural network is to minimize the cumulative error, which can be expressed as:

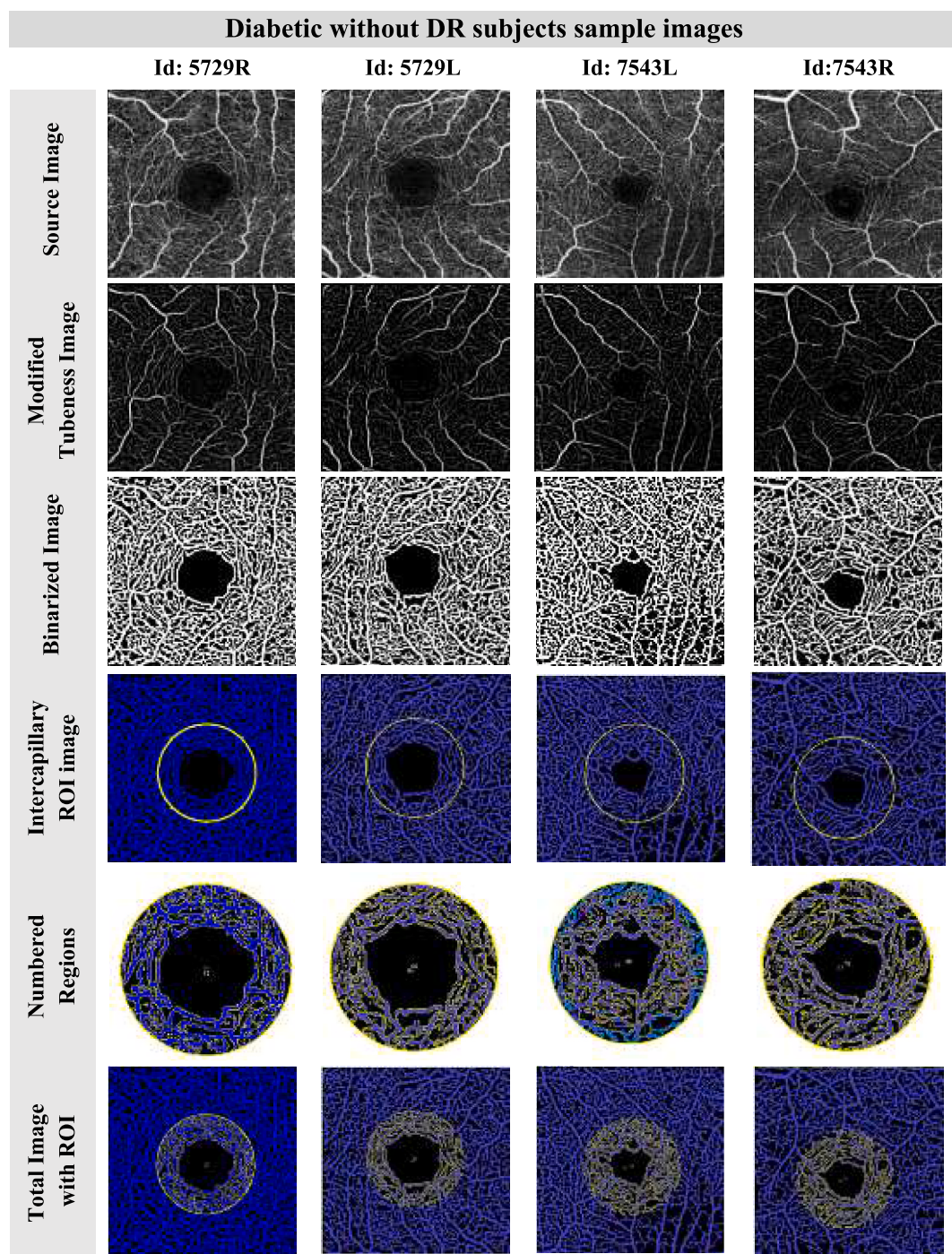


Fig. 6. Diabetic without DR subjects Sample Images.

$$E = \frac{1}{2} \sum_{i=1}^N (y_i - o_k)^2 \quad (1)$$

Where.

N is the total number of neurons, y_i is the target output, and o_k is the actual neuron output. According to the network error, weights w should be modified as:

$$w_{ij} = w_{ij} \pm \alpha x_i \quad (2)$$

Where α is the learning parameter that is constant, the sign may be positive or negative according to the resulted output and errors. There are several learning methods in neural networks [60,61]. Many

researchers as stated before used neural networks in classification applications.

4. Results and discussion

4.1. Image processing results

Image samples for Normal, Diabetic without DR, and NPDR are summarized in Fig. 5, Fig. 6 and Fig. 7.

Figs. 5–7 consist of:

1st row contains the source images.

2nd row contains the images after microvascular structure enlargement and enhancement.

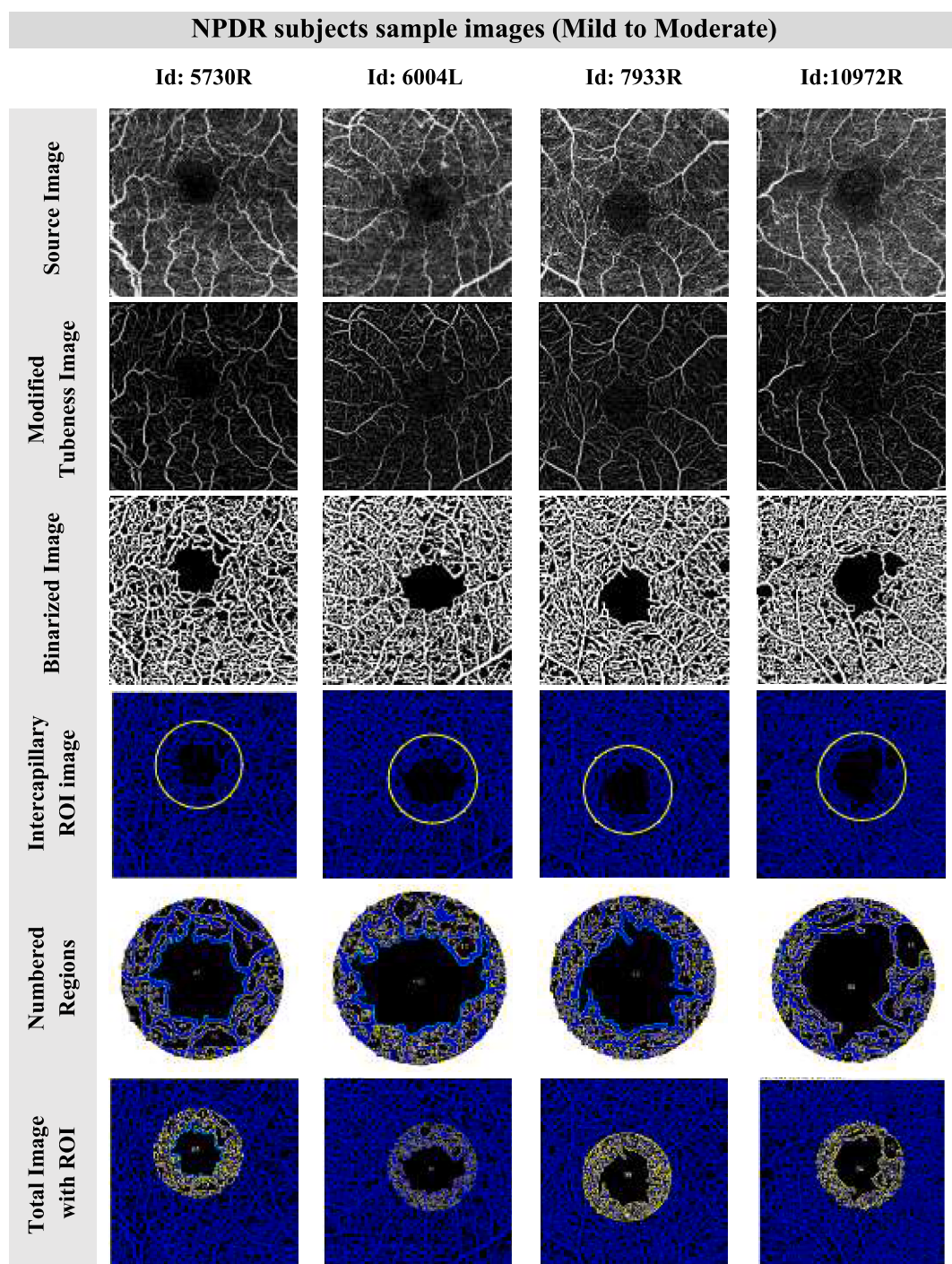


Fig. 7. Mild to Moderate NPDR subjects Sample Images.

3rd row displays the binarized shape of the microvascular structure.

4th row displays the colored binarized image with a 1.5 mm diameter circle centered at the FAZ region.

5th row displays the enlarged circle with the intercapillary regions around the FAZ region.

6th row contains the total image marked by intercapillary regions.

The FAZ regions in normal cases have more circularity shape than DWDR and DR cases. The diabetic retinopathy cases have large FAZ areas and perimeters compared to normal and DWDR cases because of the beginning of vascular malformation. The intercapillary areas are small in normal cases, while they are slightly large in DWDR due to minute microvasculature that is blocked. More gaps are introduced due

to the greater microvascular that is blocked with the creation of new microvascular abnormalities.

4.2. The demographic characteristics

The Demographic characteristics of normal and diabetic subjects are shown in [Table 1](#). One hundred eyes were examined in 40 healthy persons, 30 diabetic ones without DR, and 30 mild to moderate NPDR eyes.

From [Table 1](#), statistical analyses are conducted to assess the significance of the demographic characteristics. In this study, data are significant provided the associated *P*-value is smaller than 0.05. The

Table 1
Demographic Characteristics of the Normal and diabetic Subjects.

Characteristics	Normal (N = 40)	Diabetics without DR (DWDR) (N = 30)	Mild to moderate NPDR (N = 30)	p- value
Age (y)	51.6 ± 6.98	53.17 ± 9.5	54.7 ± 8.37	0.2974
Average ± STD				
Female/male (N)	19/21	17/13	10/20	0.2591
Laterality (RT/ LT)	17/23	19/11	16/14	0.5726

average and standard deviation of the subject ages are shown with $P > 0.2974$ ($P > 0.05$), which is statistically non-significant. Consequently, it cannot be said with certainty that the different subjects' ages affect the studied results. The female/male subjects are 46/54, with $P > 0.2591$. The laterality RT/LT is 52/48 with $P > 0.5726$. Thus, the demographic characteristics are statistically non-significant.

4.3. Image analysis results

In this section, the images will be analyzed to extract the seven features that will be used as neural network inputs. For the quantitative analysis of the intercapillary area, the mean of the 10 and 20 largest intercapillary areas are calculated, either including or excluding the FAZ region, circularity index, FAZ perimeter, and vascular density. Calculating these parameters is an important factor for measuring excess microvascular vessels in diabetic subjects. The feature-extracted results for sample image subjects are summarized in Table 2.

The normal cases either include or exclude the FAZ region have lowest areas, while the diabetic patients have medium areas and the largest areas are obtained in diabetic retinopathy patients; this means that it is a good metric to distinguish between them. In general, it is found that diabetic images include little increase in the number of intercapillary areas with random structures and capillary loss. This fact, in turn, affects the shape and the area of the FAZ region and leads to deformation in its circular shape. It is clear from the circularity coefficient, which has a minimum coefficient of 0.518 in normal cases and increased to 0.551 in diabetic without retinopathy patients, while there is less circularity in diabetic retinopathy patients with a max circularity index of 0.438.

For all subjected cases 40 normal persons, 30 diabetic patients without retinopathy, and 30 diabetic patients with retinopathy eyes, the results are summarized in Table 3.

Table 3 shows the complete subject results. The three subject types are studied by obtaining the mean of the largest 10 and 20 intercapillary

regions that lie inside a 1.5 mm circle diameter centered at the FAZ, including and excluding the FAZ region, FAZ Perimeter, FAZ circularity index, and vascular density. For comparison purposes, the three subject types are analyzed by the ANOVA (Analysis of Variances) test and have highly significant results with $P < 0.0001$ except for 20 ROI has $P < 0.0006$. It is a very encouraging result and provides a rationale for continued development.

These results in Table 3 are shown in Fig. 8. It is clear that normal eyes have the smallest areas for 10 and 20 ROI, either including or excluding the FAZ region Fig. 8(a, b, c, d); this result is due to an approximately normal distribution of microvascular vessels. These areas begin to increase in DWDR and increase more in NPDR due to little blood vessels that are blocked, and new abnormal microaneurysms that are created.

In contrast, due to the presence of new capillaries that affect the FAZ circularity shape, Non-proliferative DR has the largest FAZ perimeter 4.2732 mm and the lowest circularity index 0.3734 see Fig. 8 (e, f). The normal subjects have the lowest FAZ perimeter of 2.6773 mm and the high circularity has shape with a 0.6442 circularity index. In normal subjects, blood vessels have an approximately normal distribution with 51.54% vascular density, Fig. 8 (g). In diabetic patients without diabetic retinopathy, little blood vessels are blocked without vision effect; thus, the vascular density decreases to 46.62%. But in Non-proliferative DR

Table 3
The subjects Results.

Item	Normal	DWDR	NPDR	p- value
Mean Area (10 ROI) without FAZ (mm ²) (± std)	0.0107 (±0.0013)	0.0198 (±0.0026)	0.0246 (±0.0047)	0.0001
Mean Area (10 ROI) with FAZ (mm ²) (± std)	0.0496 (±0.078)	0.0618 (±0.016)	0.0782 (±0.0042)	0.0001
Mean Area (20 ROI) without FAZ (mm ²) (± std)	0.0081 (±0.0012)	0.01584 (±0.00225)	0.0171 (±0.0035)	0.0006
Mean Area (20 ROI) with FAZ (mm ²) (± std)	0.0287 (±0.0044)	0.0373 (±0.0078)	0.0462 (±0.0032)	0.0001
FAZ Perimeter (mm) (± std)	2.6773 (±0.2758)	3.135 (±0.5128)	4.2732 (±0.3038)	0.0001
FAZ Circularity Index (± std)	0.6442 (±0.0523)	0.5518 (±0.0816)	0.3734 (±0.0307)	0.0001
Vascular Density (%) (± std)	51.54 (±1.825)	46.62 (±1.802)	47.185 (±1.285)	0.0001

N: Normal, DWDR: Diabetic without DR and NPDR: Non-Proliferative DR, DR: Diabetic retinopathy.

Table 2
Feature extracted for the sample images.

Image Id	Status	Mean Area (10 regions) (mm ²)		Mean Area (20 regions) (mm ²)		FAZ Perimeter (mm)	FAZ Circulation Index	Vascular Density (%)
		With FAZ	Without FAZ	With FAZ	Without FAZ			
2879R	N	0.0480	0.0120	0.0280	0.0098	2.66	0.661	48.45
6961R	N	0.0360	0.0075	0.0207	0.0065	2.325	0.667	52.89
7031R	N	0.0474	0.0112	0.0274	0.0092	2.98	0.518	51.25
12203R	N	0.0670	0.0113	0.0377	0.0097	3.248	0.653	49.74
5729L	DWDR	0.0738	0.0175	0.04234	0.01397	3.66	0.54	48.12
5729R	DWDR	0.0772	0.02176	0.04517	0.01633	3.45	0.64	45.58
7543L	DWDR	0.0459	0.01756	0.02858	0.01425	2.89	0.446	46.54
7543R	DWDR	0.05037	0.02226	0.03309	0.01881	2.54	0.581	43.57
5730R	NPDR	0.0735	0.0309	0.0440	0.0224	3.55	0.438	44.35
6004L	NPDR	0.0767	0.0160	0.0418	0.0124	4.5	0.351	46.05
7933R	NPDR	0.0715	0.0156	0.0410	0.0128	4.66	0.330	47.1
10972R	NPDR	0.0840	0.0250	0.0467	0.0169	4.6	0.358	47.28

N: Normal, DWDR: Diabetic without DR and NPDR: Non-Proliferative DR, DR: Diabetic retinopathy.

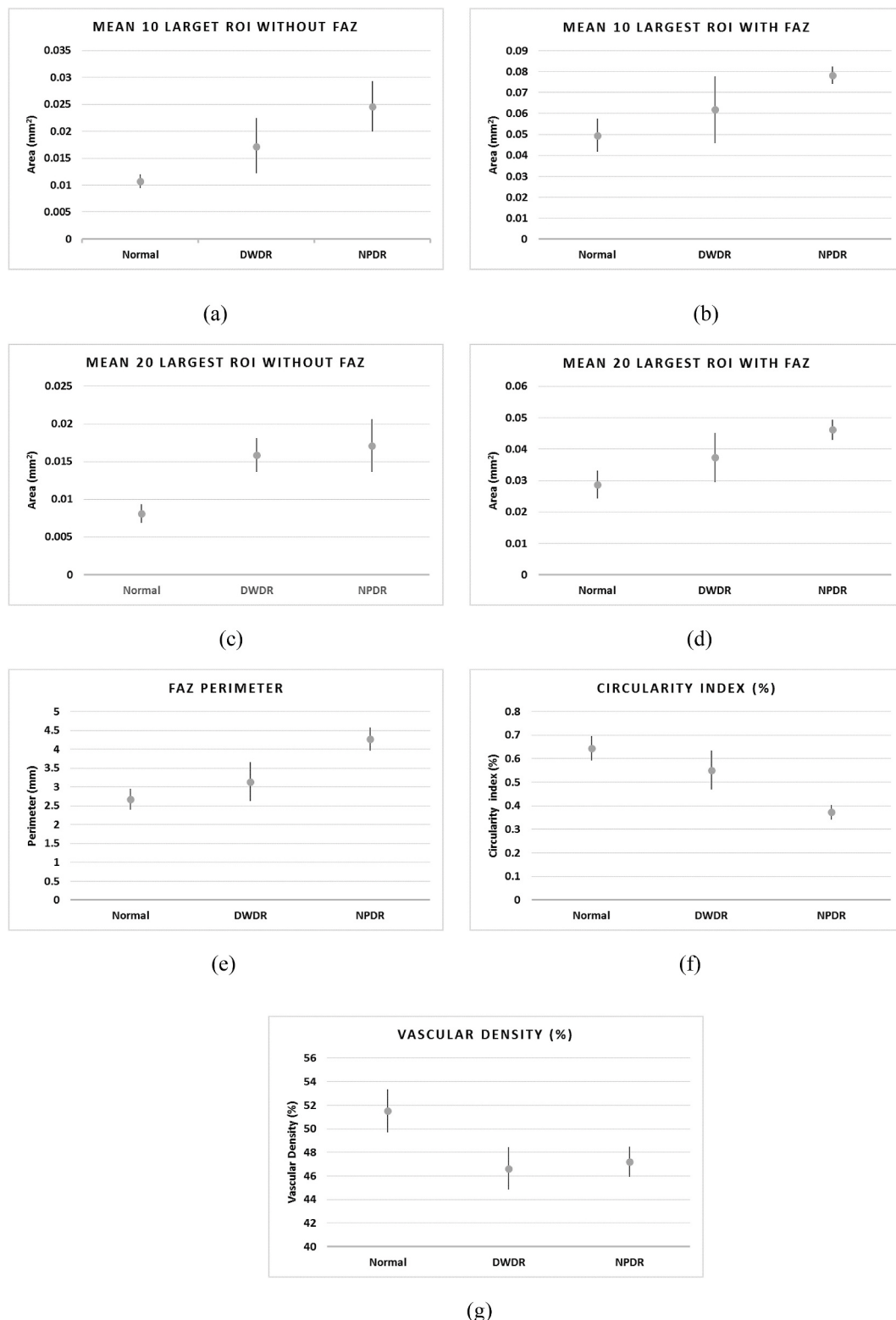


Fig. 8. Total comparison between normal, DWDR and NPDR

(mild to moderate), little new microaneurysms are created so that the vascular density increases to 47.185%.

After extracting the seven features or parameters from the subject images, four layers of an artificial neural network are used as classifiers. The network layers consist of 7, 5, 10, and 3 neurons respectively. The network performance reaches 0.0018. Only 70 sample images are used in the neural network training while the other 30 images (10 images for

each category) are used in network testing, i.e., the tested datasets contain 70 images from the training datasets and new 30 images for verifying the classification effectiveness.

4.4. Performance measures

To deduce the quality of the proposed system, several performance

Table 4
Classification Accuracy data.

Numbers	Normal	DWDR	NPDR	Total
Subjects	40	30	30	100
Correctly classified images	39	29	29	97
False classified images	1	1	1	3
Classification Accuracy = (97/100)*100 = 97%				

DWDR: Diabetic without DR and NPDR: Non-Proliferative DR, DR: diabetic retinopathy.

Table 5
Confusion Matrix normal versus diabetic.

Actual status	Classified Normal	Classified Diabetic
Normal (40)	39 TP (True Positive)	1 FN (False negative)
Diabetic (60)	2 FP (False Positive)	58 TN (True Negative)

Table 6
Confusion matrix DWDR versus NPDR.

Actual status	Classified DWDR	Classified NPDR
DWDR (30)	29 TP (True Positive)	1 FN (False negative)
NPDR (30)	1 FP (False Positive)	29 TN (True Negative)

DWDR: Diabetic without DR and NPDR: Non-Proliferative DR, DR: diabetic retinopathy.

Table 7
Sensitivity, specificity and precision parameters.

Performance Parameters	Normal vs. Diabetic	DWDR vs. NPDR
Sensitivity (%) [TP/(TP + FN)]*100	97.5	96.67
Specificity (%) [TN/(TN + FP)]*100	96.67	96.67
Precision (%) [TP/(TP + FP)]*100	95.12	96.67
Misclassification Error (%) [(FP + FN)/(TP + TN + FP + FN)]*100	3	3.33

DWDR: Diabetic without DR and NPDR: Non-Proliferative DR, DR: diabetic retinopathy.

measures can be used to assess system effectiveness. The used measures are:

- Classification accuracy: the closeness of the measurements to the desired value.
- Confusion matrix: a performance measure table, which is used to describe the performance of a classification model.
- Sensitivity: measures how positive individuals are correctly classified.
- Specificity: measures how negative individuals are correctly classified.
- Precision: how the closeness of two or more measurements are to each other.

Table 4, **Table 5**, **Table 6**, and **Table 7** summarize the performance measure results.

From **Table 4** to **Table 7**, it can be concluded that the classification accuracy of the suggested classifier method reaches 97% for 100 studied eyes. The extracted features describe precisely the morphological changes in the retina. The chosen features have different distributions and values, which differ from one stage to the other and enable the classification process.

For normal and diabetic comparison, the sensitivity was 97.5%,

specificity reached 96.67% and precision was 95.12%. While in DWRP and NPDR, the comparison sensitivity, specificity and precision reached 96.67%, 96.67%, and 96.67%, respectively. These results can be easily enhanced by increasing the number of subjects. The misclassification error has a minimum value of 3%–3.33% for both diagnosing stages.

In the end, the proposed methodology depends on OCTA image quality. In this study, the quality of the studied images ranged between 40% and 65%, which can be achieved by most OCTA instruments. The methodology limitation increases when the quality of the images is less than 35% or 30%, and poor extracted features will be obtained. Therefore, medical diagnoses may be difficult with this methodology, even for physicians.

Another approach that can be used in the classification of diabetic retinopathy is a Support Vector Machine. It is a useful approach in the case of limiting datasets. It is a supervised machine learning method, which depends on plotting the data item as a point in a dimensional space equal to the extracted features. Then it helps in determining the hyperplane that correctly differentiates the classes. However, SVM has limitations: 1) it has several key parameters that need to be set correctly to achieve the best classification results. 2) An over-fitting which may occur in case the number of features is much greater than the number of samples. 3) Long training time for large datasets. Yet, this approach may be useful in future works as a classification methodology.

5. Conclusion

A supervised machine learning based on artificial neural network as a classification tool was proposed. The subjects' eyes were imaged using OCTA. The quality of the studied images ranged between 40% and 65%. The proposed system is important as it provides an accurate, automatic, and quantitative simple method for early detection of diabetic retinopathy, where this topic was the main concern for this study. The early detection helps speed up treatments and delays diabetic-related blindness. The classification between diabetic without DR and non-proliferative retinopathy eyes achieved a 97% accuracy despite limited datasets. The diagnosis has been done by using the selecting strategy features; the selected features are the largest 10 and 20 intercapillary areas within a circle centered at FAZ with diameter 1.5 mm, either including or excluding the FAZ area region, FAZ perimeter, FAZ circularity index, and vascular density. It was shown through analysis that the usage of these selected features correlates directly to significant morphological changes in the retinal vascular system. The usage of these features as inputs in ANN is helpful in early diagnosis of DR to avoid a long and difficult course of treatment and also to avoid rapid blindness.

The proposed algorithm can be extended easily for the detection of other stages like severe NPDR and PDR. However, this study aims at detecting the early stages, which may be confused at times based on the quality of the images or multiple diagnoses to make the appropriate decision.

5.1. Future work

- Design a new Graphical User Interface (GUI) application that can extract the selected image features for early detection and diagnosis.
- Introduce the effect of multifractal analysis of the retinal vascular network in the detection and classification of the diabetic retinopathy stages.
- Use the Support Vector Machine approach in the classification of diabetic retinopathy stages.

Declaration of competing interest

The authors declare that they have no known competing financial interests or personal relationships that could have appeared to influence the work reported in this paper.

Acknowledgement

The author would like to thank Elshaimaa Amin, medical analysis specialist, Ophthalmology Center, Mansoura University-Egypt for her support in obtaining OCTA images.

Appendix A. Supplementary data

Supplementary data to this article can be found online at <https://doi.org/10.1016/j imu.2020.100390>.

References

- [1] Jiang F, Jiang Y, Zhi H, Dong Y, Li H, Ma S, Wang Y, Dong Q, Shen H, Wang Y. Artificial intelligence in healthcare: past, present and future. *Stroke Vasc Neurol* 2017;2:230–43. <https://doi.org/10.1136/svn-2017-000101>.
- [2] Chan Y-K, Chen Y-F, Pham T, Chang W, Hsieh M-Y. Artificial intelligence in medical applications. *J Healthc Eng* 2018;2018:1–2. <https://doi.org/10.1155/2018/482785>.
- [3] Kashyap Abhishek. Artificial intelligence & medical DiagnosisNo title. Scholars J Appl Med Sci 2018;6:4982–5. <https://doi.org/10.21276/sjams.2018.6.12.61>.
- [4] Kim JK, Choi MJ, Lee JS, Hong JH, Kim C-S, Il Seo S, Jeong CW, Byun S-S, Koo KC, Chung BH, Park YH, Lee JY, Choi IY. A deep belief network and dempster-shafer-based multiclassifier for the pathology stage of prostate cancer. *J. Healthc. Eng.* 2018;1–8. <https://doi.org/10.1155/2018/4651582>. 2018.
- [5] Kann SA Benjamin H, Thompson Reid, Thomas PhDCharles R. Adam dicker, artificial intelligence in oncology: current applications and future directions. *Oncol J* 2019;33:46–53.
- [6] Ho D. Artificial intelligence in cancer therapy. *Science* 2020;367(80):982–3. <https://doi.org/10.1126/science.aaz3023>.
- [7] Coward LA. Brain anatomy and artificial intelligence. 2011. p. 255–68. https://doi.org/10.1007/978-3-642-22887-2_27.
- [8] Fellous J-M, Sapiro G, Rossi A, Mayberg H, Ferrante M. Explainable artificial intelligence for neuroscience: behavioral neurostimulation. *Front Neurosci* 2019;13. <https://doi.org/10.3389/fnins.2019.01346>.
- [9] Fang L, Cunefare D, Wang C, Guymer RH, Li S, Farsiu S. Automatic segmentation of nine retinal layer boundaries in OCT images of non-exudative AMD patients using deep learning and graph search. *Biomed Optic Express* 2017;8:2732. <https://doi.org/10.1364/BOE.8.0002732>.
- [10] Guo Y, Camino A, Wang J, Huang D, Hwang TS, Jia Y. MEDnet, a neural network for automated detection of avascular area in OCT angiography. *Biomed Optic Express* 2018;9:5147. <https://doi.org/10.1364/BOE.9.0005147>.
- [11] Arcadu F, Benmansour F, Maunz A, Michon J, Haskova Z, McClintock D, Adamis AP, Willis JR, Prunotto M. Deep learning predicts OCT measures of diabetic macular thickening from color fundus photographs. *Investig Ophthalmol Vis Sci* 2019;60:852. <https://doi.org/10.1167/ios.18-25634>.
- [12] Benjamins JW, Hendriks T, Knuuti J, Juarez-Orozco LE, van der Harst P. A primer in artificial intelligence in cardiovascular medicine, Netherlands Hear. J 2019;27:392–402. <https://doi.org/10.1007/s12471-019-1286-6>.
- [13] Kagiyama N, Shrestha S, Farjo PD, Sengupta PP. Artificial intelligence: practical primer for clinical research in cardiovascular disease. *J Am Heart Assoc* 2019;8. <https://doi.org/10.1161/JAHA.119.012788>.
- [14] da Marvao A, Dawes TJW, O'Regan DP. Artificial intelligence for cardiac imaging-genetics research. *Front Cardiovasc Med* 2020;6. <https://doi.org/10.3389/fcvm.2019.00195>.
- [15] Ozkan IA, Koklu M, Sert IU. Diagnosis of urinary tract infection based on artificial intelligence methods. *Comput Methods Progr Biomed* 2018;166:51–9. <https://doi.org/10.1016/j.cmpb.2018.10.007>.
- [16] Pesapane F, Codari M, Sardanelli F. Artificial intelligence in medical imaging: threat or opportunity? Radiologists again at the forefront of innovation in medicine. *Eur Radiol Exp* 2018;2:35. <https://doi.org/10.1186/s41747-018-0061-6>.
- [17] Bahado-Singh RO, Sonek J, McKenna D, Cool D, Aydas B, Turkoglu O, BJORNDHAL T, Mandal R, Wishart D, Friedman P, Graham SF, Yilmaz A. Artificial intelligence and amniotic fluid multiomics: prediction of perinatal outcome in asymptomatic women with short cervix. *Ultrasound Obstet. Gynecology* 2019;54:110–8. <https://doi.org/10.1002/uog.20168>.
- [18] Lakshmi BN, Indumathi TS, Ravi N. An hybrid approach for prediction based health monitoring in pregnant women. *Procedia Technol* 2016;24:1635–42. <https://doi.org/10.1016/j.protcy.2016.05.171>.
- [19] Le Berre C, Sandborn WJ, Aridhi S, Devignes M-D, Fournier L, Smaïl-Tabbone M, Danese S, Peyrin-Biroulet L. Application of artificial intelligence to gastroenterology and hepatology. *Gastroenterology* 2020;158:76–94. <https://doi.org/10.1053/j.gastro.2019.08.058>. e2.
- [20] He YS, Su JR, Li Z, Zuo XL, Li YQ. Application of artificial intelligence in gastrointestinal endoscopy. *J Dig Dis* 2019;20:623–30. <https://doi.org/10.1111/1751-2980.12827>.
- [21] Catherwood PA, Rafferty J, McLaughlin J. Artificial intelligence for long-term respiratory disease management. 2018. <https://doi.org/10.14236/ewic/HCI2018.65>.
- [22] Labaki WW, Han MK. Artificial intelligence and chest imaging. Will deep learning make us smarter? *Am J Respir Crit Care Med* 2018;197:148–50. <https://doi.org/10.1164/rccm.201709-1879ED>.
- [23] Hassanzadeh P, Atayabi F, Dinarvand R. The significance of artificial intelligence in drug delivery system design. *Adv Drug Deliv Rev* 2019;151–152:169–90. <https://doi.org/10.1016/j.addr.2019.05.001>.
- [24] Schork NJ. Artificial intelligence and personalized medicine. 2019. p. 265–83. https://doi.org/10.1007/978-3-030-16391-4_11.
- [25] Allen F, Crepaldi L, Alsinet C, Strong AJ, Kleshchhevnikov V, De Angeli P, Páleníková P, Khodak A, Kiselev V, Kosicki M, Bassett AR, Harding H, Galanty Y, Muñoz-Martínez F, Metzakopian E, Jackson SP, Parts L. Predicting the mutations generated by repair of Cas9-induced double-strand breaks. *Nat Biotechnol* 2019;37:64–72. <https://doi.org/10.1038/nbt.4317>.
- [26] Wang W, Lo A. Diabetic retinopathy: pathophysiology and treatments. *Int J Mol Sci* 2018;19:1816. <https://doi.org/10.3390/ijms19061816>.
- [27] Romero-Aroca P, Baget-Bernaldiz M, Pareja-Rios A, Lopez-Galvez M, Navarro-Gil R, Verges R. Diabetic macular edema pathophysiology: vasogenic versus inflammatory. *J Diabetes Res* 2016;1:1–17. <https://doi.org/10.1155/2016/2156273>. 2016.
- [28] Brownlee M. The pathobiology of diabetic complications: a unifying mechanism. *Diabetes* 2005;54:1615–25. <https://doi.org/10.2337/diabetes.54.6.1615>.
- [29] Bek T. Diameter changes of retinal vessels in diabetic retinopathy. *Curr Diabetes Rep* 2017;17:82. <https://doi.org/10.1007/s11892-017-0909-9>.
- [30] Tarr JM, Kaul K, Chopra M, Kohner EM, Chibber R. Pathophysiology of diabetic retinopathy. *ISRN Ophthalmol* 2013;1:1–13. <https://doi.org/10.1155/2013/343560>. 2013.
- [31] Kern TS, Antonetti DA, Smith LEH. Pathophysiology of diabetic retinopathy: contribution and limitations of laboratory research. *Ophthalmic Res* 2019;62:196–202. <https://doi.org/10.1159/oos.000000026>.
- [32] Wong TY, Sun J, Kawasaki R, Ruamviboonsuk P, Gupta N, Lansing VC, Maia M, Mathenge W, Moreker S, Mugit MMK, Resnikoff S, Verdaguer J, Zhao P, Ferris F, Aiello LP, Taylor HR. Guidelines on diabetic eye care. *Ophthalmology* 2018;125:1608–22. <https://doi.org/10.1016/j.jophtha.2018.04.007>.
- [33] Windisch R, Windisch BK, Cruess AF. Use of fluorescein and indocyanine green angiography in polypoidal choroidal vasculopathy patients following photodynamic therapy. *Can J Ophthalmol* 2008;43:678–82. <https://doi.org/10.3129/i08-153>.
- [34] Teussink MM, Breukink MB, van Grinsven MJJP, Hoyng CB, Klevering BJ, Boon CJF, de Jong EK, Theelen T. OCT angiography compared to fluorescein and indocyanine green angiography in chronic central serous chorioretinopathy. *Investig Ophthalmol Vis Sci* 2015;56:5229. <https://doi.org/10.1167/iovs.15-17140>.
- [35] de Carlo TE, Romano A, Waheed NK, Duke JS. A review of optical coherence tomography angiography (OCTA). *Int J Retin Vitr* 2015;1:5. <https://doi.org/10.1186/s40942-015-0005-8>.
- [36] Mehrotra N, Nagpal M, Khandelwal J, Juneja R. Panoramic optical coherence tomography angiography features in acute zonal occult outer retinopathy. *Indian J Ophthalmol* 2018;66:1856. https://doi.org/10.4103/ijo.IJO_826_18.
- [37] Tey KY, Teo K, Tan ACS, Devarajan K, Tan B, Tan J, Schmetterer L, Ang M. Optical coherence tomography angiography in diabetic retinopathy: a review of current applications. *Eye Vis* 2019;6:37. <https://doi.org/10.1186/s40662-019-0160-3>.
- [38] Biran K, Sobie A, Almazroe C, Raahemifar AV. Automatic detection and classification of diabetic retinopathy using retinal fundus images. *Int J Comput Inf Eng* 2016;10:1308–11.
- [39] Kamaladevi T, SnehaRupa M, Sowmya S. Automatic detection of diabetic retinopathy in large scale retinal images. *Int J Pure Appl Math* 2018;119:14181–9.
- [40] Saleh MD, Eswaran C. An automated decision-support system for non-proliferative diabetic retinopathy disease based on MAs and HAs detection. *Comput Methods Progr Biomed* 2012;108:186–96. <https://doi.org/10.1016/j.cmpb.2012.03.004>.
- [41] Wu B, Zhi W, Shi F, Zhi S, Chen X. Automatic detection of microaneurysms in retinal fundus images. *Comput Med Imag Graph* 2017;55:106–12. <https://doi.org/10.1016/j.compimedimag.2016.08.001>.
- [42] Gargya R, Leng T. Automated identification of diabetic retinopathy using deep learning. *Ophthalmology* 2017;124:962–9. <https://doi.org/10.1016/j.jophtha.2017.02.008>.
- [43] Hemanth DJ, Deperlioglu O, Kose U. An enhanced diabetic retinopathy detection and classification approach using deep convolutional neural network. *Neural Comput Appl* 2020;32:707–21. <https://doi.org/10.1007/s00521-018-03974-0>.
- [44] Gao Z, Li J, Guo J, Chen Y, Yi Z, Zhong J. Diagnosis of diabetic retinopathy using deep neural networks. *IEEE Access* 2019;7:3360–70. <https://doi.org/10.1109/ACCESS.2018.2888639>.
- [45] Sahlsten J, Jaskari J, Kivinen J, Turunen L, Jaanio E, Hietala K, Kaski K. Deep learning fundus image analysis for diabetic retinopathy and macular edema grading. *Sci Rep* 2019;9:10750. <https://doi.org/10.1038/s41598-019-47181-w>.
- [46] Gulshan V, Peng L, Coram M, Stumpf MC, Wu D, Narayanaswamy A, Venugopalan S, Widner K, Madams T, Cuadros J, Kim R, Raman R, Nelson PC, Mega JL, Webster DR. Development and validation of a deep learning algorithm for detection of diabetic retinopathy in retinal fundus photographs. *J Am Med Assoc* 2016;316:2402. <https://doi.org/10.1001/jama.2016.17216>.
- [47] Zago GT, Andreão RV, Dorizzi B, Teatini Salles EO. Diabetic retinopathy detection using red lesion localization and convolutional neural networks. *Comput Biol Med* 2020;116:103537. <https://doi.org/10.1016/j.combiomed.2019.103537>.
- [48] Lam T, Carson, Yi Darvin, Guo Margaret, Lindsey. Automated detection of diabetic retinopathy using deep learning. *AMIA Summits Transl Sci Proc* 2017:147–55. 2018.

- [49] Ghosh R, Ghosh K, Maitra S. Automatic detection and classification of diabetic retinopathy stages using CNN. In: 2017 4th int. Conf. Signal process. Integr. Networks. IEEE; 2017. p. 550–4. <https://doi.org/10.1109/SPIN.2017.8050011>.
- [50] Xu K, Feng D, Mi H. Deep convolutional neural network-based early automated detection of diabetic retinopathy using fundus image. *Molecules* 2017;22:2054. <https://doi.org/10.3390/molecules22122054>.
- [51] Wang X, Lu Y, Wang Y, Chen W-B. Diabetic retinopathy stage classification using convolutional neural networks. In: IEEE int. Conf. Inf. Reuse integr. IEEE; 2018. p. 465–71. <https://doi.org/10.1109/IRI.2018.00074>. 2018.
- [52] Pratt H, Coenen F, Broadbent DM, Harding SP, Zheng Y. Convolutional neural networks for diabetic retinopathy. *Procedia Comput Sci* 2016;90:200–5. <https://doi.org/10.1016/j.procs.2016.07.014>.
- [53] Jahiruzzaman M, Hossain ABMA. Detection and classification of diabetic retinopathy using K-means clustering and fuzzy logic. In: 2015 18th int. Conf. Comput. Inf. Technol. IEEE; 2015. p. 534–8. <https://doi.org/10.1109/ICCI.2015.7488129>.
- [54] Leontidis G, Al-Diri B, Hunter A. A new unified framework for the early detection of the progression to diabetic retinopathy from fundus images. *Comput Biol Med* 2017;90:98–115. <https://doi.org/10.1016/j.combiomed.2017.09.008>.
- [55] Rahim SS, Palade V, Shuttleworth J, Jayne C. Automatic screening and classification of diabetic retinopathy and maculopathy using fuzzy image processing. *Brain Informatics* 2016;3:249–67. <https://doi.org/10.1007/s40708-016-0045-3>.
- [56] Olaniyi A, Ebenezer, Adekunle Adefemi, Oyedotun Oyebade, Khashman. Diabetic retinopathy diagnosis using neural network ArbitrationNo title. *Bull Transilv Univ Brasov – Ser III Math Inform Phys* 2017;10:179–92.
- [57] Welikala RA, Fraz MM, Dehmehki J, Hoppe A, Tah V, Mann S, Williamson TH, Barman SA. Genetic algorithm based feature selection combined with dual classification for the automated detection of proliferative diabetic retinopathy. *Comput Med Imag Graph* 2015;43:64–77. <https://doi.org/10.1016/j.compmedimag.2015.03.003>.
- [58] Topcon (nd. <https://www.topcon-medical.eu/eu/products/382-dri-oct-triton-swept-source-oct.html#general>.
- [59] Krawitz BD, Mo S, Geyman LS, Agemy SA, Scripsmea NK, Garcia PM, Chui TYP, Rosen RB. Acircularity index and axis ratio of the foveal avascular zone in diabetic eyes and healthy controls measured by optical coherence tomography angiography. *Vision Res* 2017;139:177–86. <https://doi.org/10.1016/j.visres.2016.09.019>.
- [60] Wilamowski B. Neural network architectures and learning algorithms. *IEEE Ind Electron Mag* 2009;3:56–63. <https://doi.org/10.1109/MIE.2009.934790>.
- [61] Dario Baptista F, Rodrigues S, Morgado-Dias F. Performance comparison of ANN training algorithms for classification. In: IEEE 8th int. Symp. Intell. Signal process., IEEE, 2013; 2013. p. 115–20. <https://doi.org/10.1109/WISP.2013.6657493>.